The Influence of Hypochlorite-Based Disinfectants on the Pitting Corrosion of Welded Joints of 316L Stainless Steel Dairy Reactor

Boguslaw Pierozynski[1] and Ireneusz M. Kowalski[2]

[1] Department of Chemistry, Faculty of Environmental Management and Agriculture, University of Warmia and Mazury in Olsztyn, Plac Lodzki 4, 10-957 Olsztyn, Poland
[2] Department of Rehabilitation, Faculty of Medical Sciences, University of Warmia and Mazury in Olsztyn, Zolnierska 14C Street, 10-561 Olsztyn, Poland
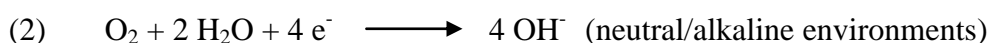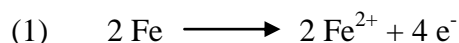[*]E-mail: bogpierozynski@yahoo.ca

The present paper reports on the investigation of a pitting corrosion phenomenon, observed in multiple locations around the welding zone of a dairy industrial reactor, made of highly corrosion-resistant 316L stainless steel (SS) material. A common practice in dairy plants involves regular disinfection of all production equipment, typically by means of hypochlorite-based disinfecting reagents. At elevated temperatures, hypochlorites can produce (via a disproportionation reaction) very aggressive chloride anions, which are able to effectively damage the passive layer present on the surface of stainless steel material, thus inducing pitting corrosion. In the present work, the corrosion process (evaluated by means of microstructural and electrochemical techniques) became greatly enhanced by improperly carried-out welding procedures, which resulted in metallurgically in-homogeneous SS material with partially defected passive layer.

1. INTRODUCTION

This work is concerned with a significant pitting corrosion problem that was observed within the welding zone of a 316L stainless steel (SS)-made dairy industrial reactor, just after 12 months of its initial installation. During its service, the production reactor was periodically subjected to sanitization procedure, carried-out by means of commercially available, hypochlorite-based disinfecting reagents, where the concentration of ClO^- ion in a base disinfectant was ≤ 15 wt. %.

Pitting of stainless steel is a form of localized corrosion attack, caused by a breakdown of the thin passive oxide film that otherwise protects material from the corrosion environment. In the presence of aggressive anions, especially Cl^-, but also Br^-, $S_2O_3^{2-}$ or ClO^-, the passive film undergoes local damage, which initiates the process of pitting. Once a pit is formed, an active-passive cell becomes established with potential difference as high as 0.5 V. The resultant high current-density is accompanied by a significant corrosion rate of an anode (pit) while the alloy surface immediately surrounding the pit forms an effective cathode [1-3]. The electrode reactions are represented by: anodic oxidation of metal inside the pit (anode) and e.g. cathodic reduction of oxygen on the surface of passivated metal (cathode), as shown in equations 1 and 2 below, correspondingly:

$$(1) \qquad 2\,Fe \longrightarrow 2\,Fe^{2+} + 4\,e^-$$

$$(2) \qquad O_2 + 2\,H_2O + 4\,e^- \longrightarrow 4\,OH^- \text{ (neutral/alkaline environments)}$$

In addition, in the presence of chloride ions, the current flow causes these ions to enter the pit and form concentrated solution of $FeCl_2$ that undergoes hydrolysis (equation 3), leading to acidification of the solution inside the pit and thus to further increase of the corrosion rate. Then, the corrosion process becomes autocatalytic and the pit growth proceeds in a perpendicular direction to the metal surface, which finally causes perforation of the material.

$$(3) \qquad FeCl_2 + 2\,H_2O \longrightarrow Fe(OH)_2\downarrow + 2\,HCl$$
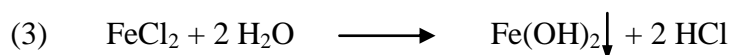
For stainless steel materials, development of pits is usually enhanced at metallurgically heterogeneous surfaces, e.g. at the austenite/ferrite interfaces, local inclusions and chromium-depleted regions (sometimes being a result of inappropriate welding procedures). The passive layers formed on such surfaces are irregular and often defected, which promotes the process of pitting corrosion [4, 5].

Hypochlorite-based disinfectants (e.g. "Divosan Hypochlorite", "Endurochlor" or "Easyfoam" of Johnson Diversey [6]) are often used in dairy plants for periodic disinfection of all production equipment, as well as production rooms. Disinfecting properties of hypochlorites are based on the release of oxygen upon their decomposition (equation 4):

$$(4) \qquad 2ClO^- \longrightarrow 2Cl^- + O_2\uparrow$$
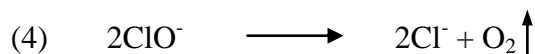
In addition, at elevated temperatures (above *ca.* 40° C) hypochlorite ions can undergo disproportionation reaction [7, 8] to form chlorate and chloride ions in reaction 5 below:

$$(5) \qquad 3ClO^- \longrightarrow ClO_3^- + 2Cl^-$$
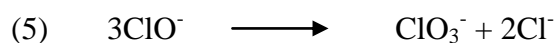
Such *in-situ* produced Cl^- ion creates ideal conditions for initiation of the process of pitting corrosion. Potential development of the corrosion process within welded zones of stainless steel material (e.g. 316L SS) is then strongly dependent on the combination of two major factors, namely:

    a)   employment of appropriate welding practices for stainless steel material and

    b)   application of manufacturer-approved procedures for sanitization processes, especially with respect to: temperature, pH, concentration and residence time of a sanitizing reagent.

2. EXPERIMENTAL

A portable, *Spectroport* metal analyzer (with Ar-based spark discharge mode) was employed to carry-out elemental analysis of virgin and welded-zone SS material specimens, while microscopic investigations were conducted by means of high resolution Zeiss *Axioscop 40* optical microscope. All examined SS samples were prepared through a sequence of mechanical polishing procedures with SiC emery papers (up to 800 grit), following final polishing with 3 and 1μm polycrystalline diamond suspensions (Metalogis, Poland), using BAS (MF-1040) polishing cloth. Such-prepared specimens were then rinsed with ultra-pure water of 18.2 MΩ cm resistivity (supplied by a Direct-Q3 UV water purification system from Millipore) and ethanol (p.a., ACS reagent). Furthermore, the samples selected for microstructural observations were additionally etched by means of the so-called *Mi16Fe* reagent (composition: 1 vol. % HNO_3 + 2 vol. % HF + 3 vol. % glycerin). In addition, in order to improve the corrosion performance of the welded-joint material, selected 316L SS plate was subjected to a passivation treatment in 25 vol. % HNO_3 (for 30 minutes at 60 ^{o}C).

Electrochemical corrosion studies employed in this work involved application of potentiodynamic Tafel (initiated after 2 hours of an open-circuit conditioning, carried-out at a sweep-rate of 0.5 mV s^{-1}) and linear polarization (LP) techniques. All measurements were conducted at room temperature by means of the *Solartron* 12,608W Full Electrochemical System, consisting of 1260A frequency response analyzer (FRA) and 1287A electrochemical interface (EI). The voltammetric polarizations were performed over controlled ranges of the working-electrode (316L SS) potential. The instrument was handled by *Corrware 2.9* software for Windows (Scribner Associates, Inc.). Presented results were obtained through selection of representative (or via averaging multiple), independent measurements, performed at selected locations of the stainless steel plates' surface. The LP data analysis was performed with *Corrview 2.9* software package.

Aqueous, 1.0 mol dm^{-3} NaCl solutions of pH 6.5 and 2.0 (the latter adjusted through addition of ultra-pure H_2SO_4, Fluka) were prepared from high purity NaCl reagent (POCH- Polish Chemical Compounds, pure, p.a.) using ultra-pure water from the Millipore system. Atmospheric oxygen was removed from solution before each experiment by bubbling with high-purity Ar (Linde, 6.0 grade). During the experiments, the argon gas flow was usually kept above the solutions.

An electrochemical cell, made all of Teflon, was used during the course of this work. The cell comprised three electrodes, namely: a 316L SS circular (1.5 cm diameter) working electrode, enclosed within a rubber o-ring on the surface of 8 mm thick stainless steel plate (see later Fig. 4), an Ag/AgCl (BAS, 3.5 mol dm^{-3} KCl) electrode as reference and a Pt counter electrode (0.5 mm diameter coiled Pt wire, BAS). Prior to each series of experiments, the electrochemical cell was taken apart, thoroughly rinsed with Millipore ultra-pure water and finally with ethanol (ACS reagent, 96 vol. %).

3. RESULTS AND DISCUSSION

3.1 Elemental composition and microstructure analysis of 316L stainless steel materials

Table 1 below presents the results of elemental composition, carried-out for both virgin and welded-joint 316L stainless steel materials.

Table 1. Evaluation of chemical composition of 316L SS materials.

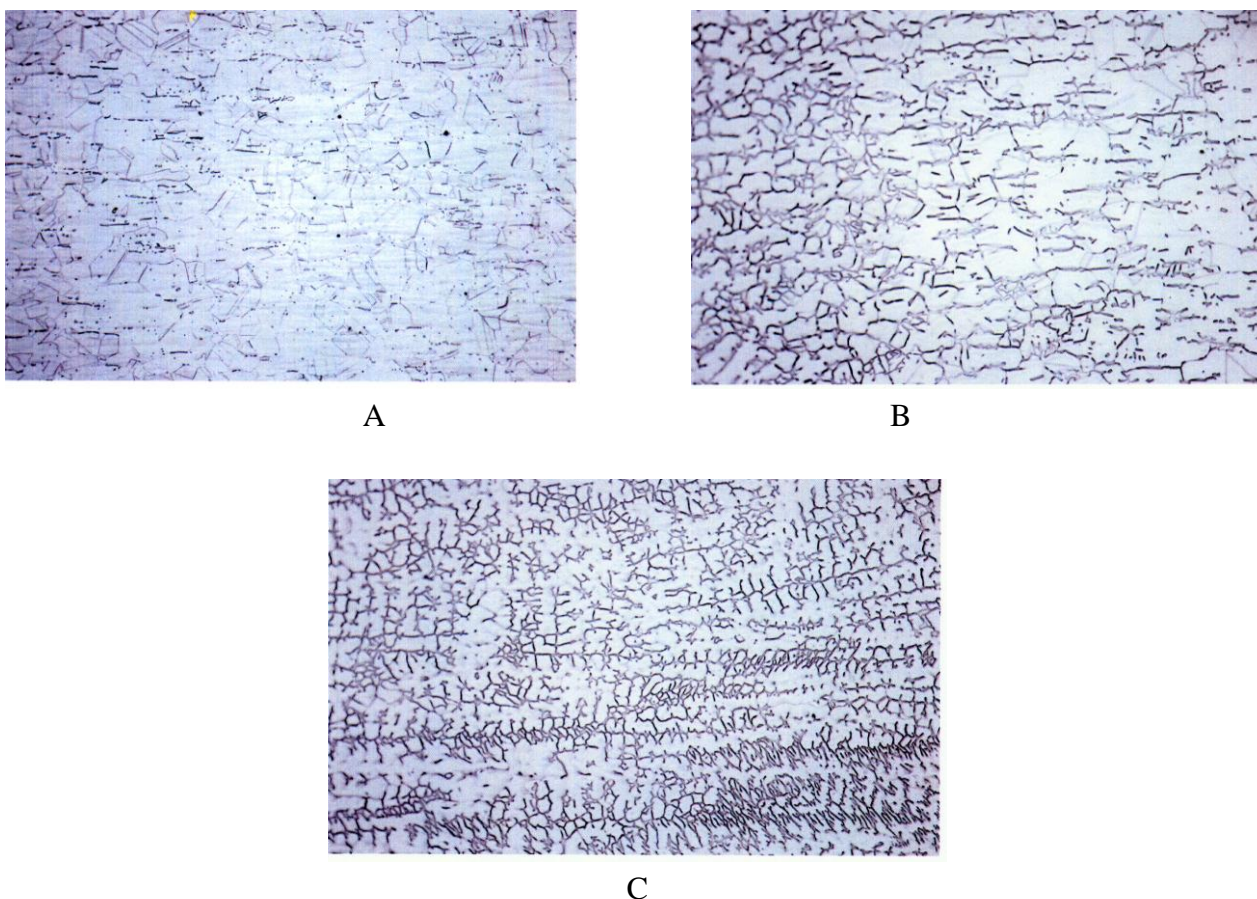| Material	Elemental content %					
	C	Si	Mn	Mo	Cr	Ni
Virgin clad	0.03	0.40	1.31	1.92	17.05	9.96
Welded joint	0.03	0.59	1.43	2.10	17.75	11.08
316L SS: ASTM A240 ASTM A666 DIN 1.4404	< 0.03	< 0.75	< 2.00	2.0-3.0	16.0-18.0	10.0-14.0

A

B

C

Figure 1. a) Cross-sectional microstructure (at 200x magnification) of virgin 316L SS (8 mm thick) clad material, b) Cross-sectional microstructure (at 200x magnification) of 316L SS welded-joint (8 mm thick) material: heat-affected zone, c) Cross-sectional microstructure (at 200x magnification) of 316L SS welded-joint (8 mm thick) material: weld area.

It can be seen there that the variation of elemental composition (with respect to the content of: C, Si, Mn, Mo, Cr and Ni elements in an alloy) for these two materials is clearly insignificant. In addition, these two alloy compositions fit very well that of a typical 316L type SS material (Table 1).

The microstructure of the virgin 316L SS material consists of an austenitic structure with a small amount (*ca.* 1 %) of δ-ferrite (see Fig. 1a above). On the other hand, austenitic microstructures of the welded-joint material are supplemented with a significant amount of δ-ferrite [about 8 and 15 % for heat-affected zone (HAZ) and weld area, correspondingly]. The δ-ferrite bands are distributed around the austenite grain boundaries, which can be seen in Figs. 1b and 1c for the HAZ and the weld, respectively.

3.2 Electrochemical characterization of pitting corrosion phenomenon

Regular application of hypochlorite-based sanitization procedure to disinfect the 316L SS-made dairy production reactor resulted in significant pitting corrosion (disclosed as micro-pit clusters, localized around the welding zone of the reactor, see Fig. 2 as an example).
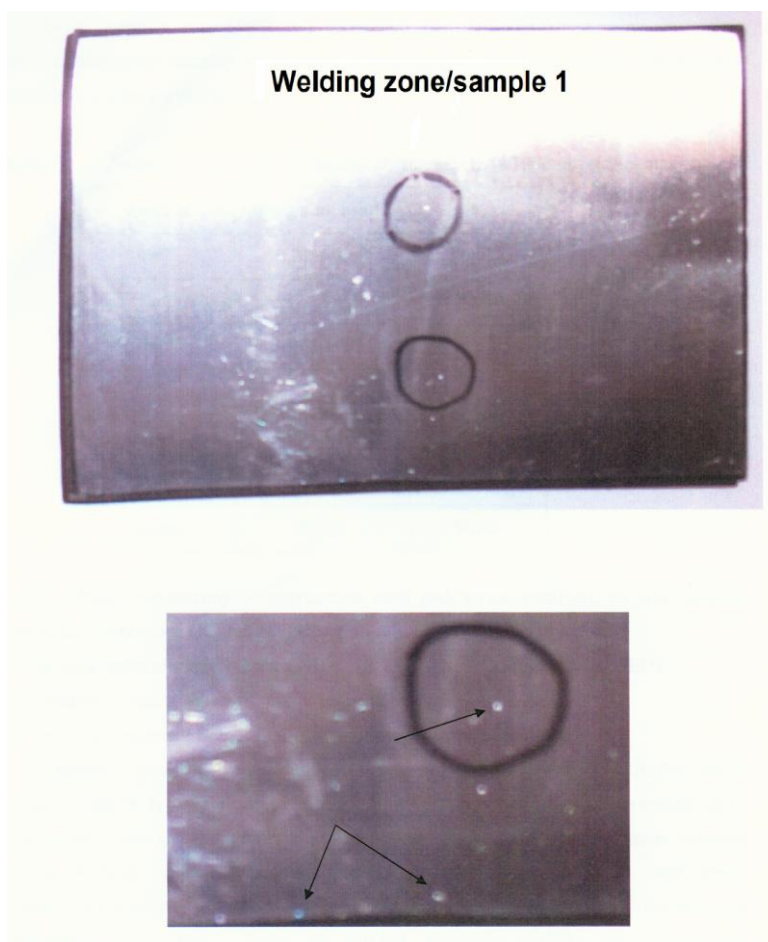

Figure 2. Corrosion micro-pits, observed on the fragment of inner surface of a 316L SS-made dairy production reactor, over its welding zone.

The pitting occurred in just about 12 months from the reactor commissioning; however, no sign of clad perforation was observed. Although the reactor end user confirmed that the sanitization process strictly followed the procedures of the disinfectant manufacturer (Johnson Diversey), no access to the sanitizing solution/procedure was permitted.
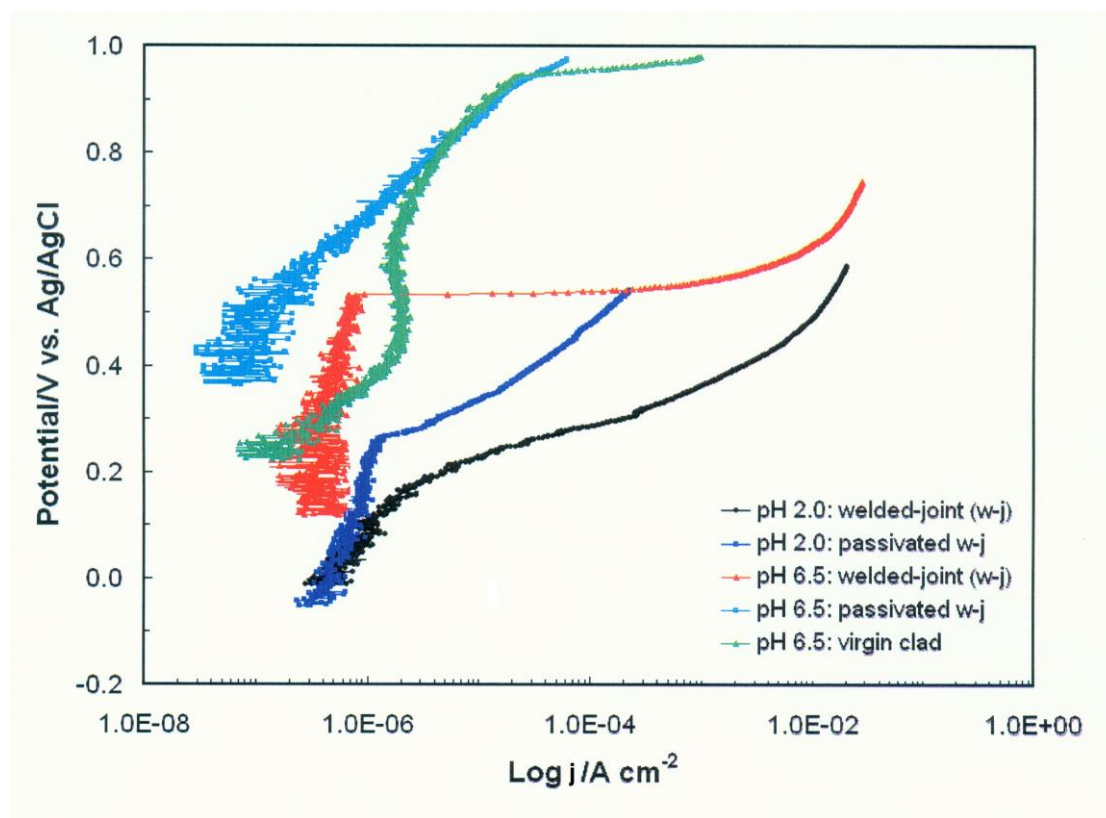

Figure 3. Anodic polarization curves for the stated 316L SS materials, in contact with 1.0 mol dm^{-3} NaCl (at pH 2.0 and 6.5), recorded at a sweep rate of 0.5 mV s^{-1}.

Fig. 3 presents potentiodynamic anodic polarization curves of 316L weldment (HAZ; both untreated and surface-passivated) and virgin clad materials, performed in contact with 1.0 mol dm^{-3} NaCl, at pH 2.0 and 6.5 values. The process of pitting was found to be strongly pH-dependent. Thus, the 316L welded-joint material at pH 6.5 exhibited significantly broader passive range and radically higher value (by *ca.* 350 mV) of pitting potential, E_{pit} (potential at which a rapid increase of current-density occurs, due to the passive layer breakdown) than the corresponding parameters obtained at pH 2.0 (see Fig. 3). Moreover, an employed surface passivation treatment significantly improved the corrosion performance of the welded-joint SS material, at both studied pHs. The above is revealed in a significant shift of the pitting potential towards more positive values, as well as that of the passive potential range to lower current-densities. In addition, the corrosion potential also underwent a considerable shift in result of the surface passivation (by *ca.* + 200 mV at pH 6.5). On the other hand, the performance of the 316L virgin clad material is superior to that exhibited by the unprocessed welded-joint specimen at pH 6.5, where the pitting potential for the former SS sample becomes

significantly shifted (by over 400 mV) towards more positive potentials, as compared to that for the latter one (see Fig. 3 again). As an effect of extended anodic polarization (beyond the pitting potential), the surface of all working electrodes became covered by clusters of micro-pits, which can clearly be seen in Fig. 4 below. The anodic polarization results obtained in this work are in agreement with those previously reported on the pitting performance of 316L (or similar) stainless steel materials in NaCl-based electrolytes [9-12].
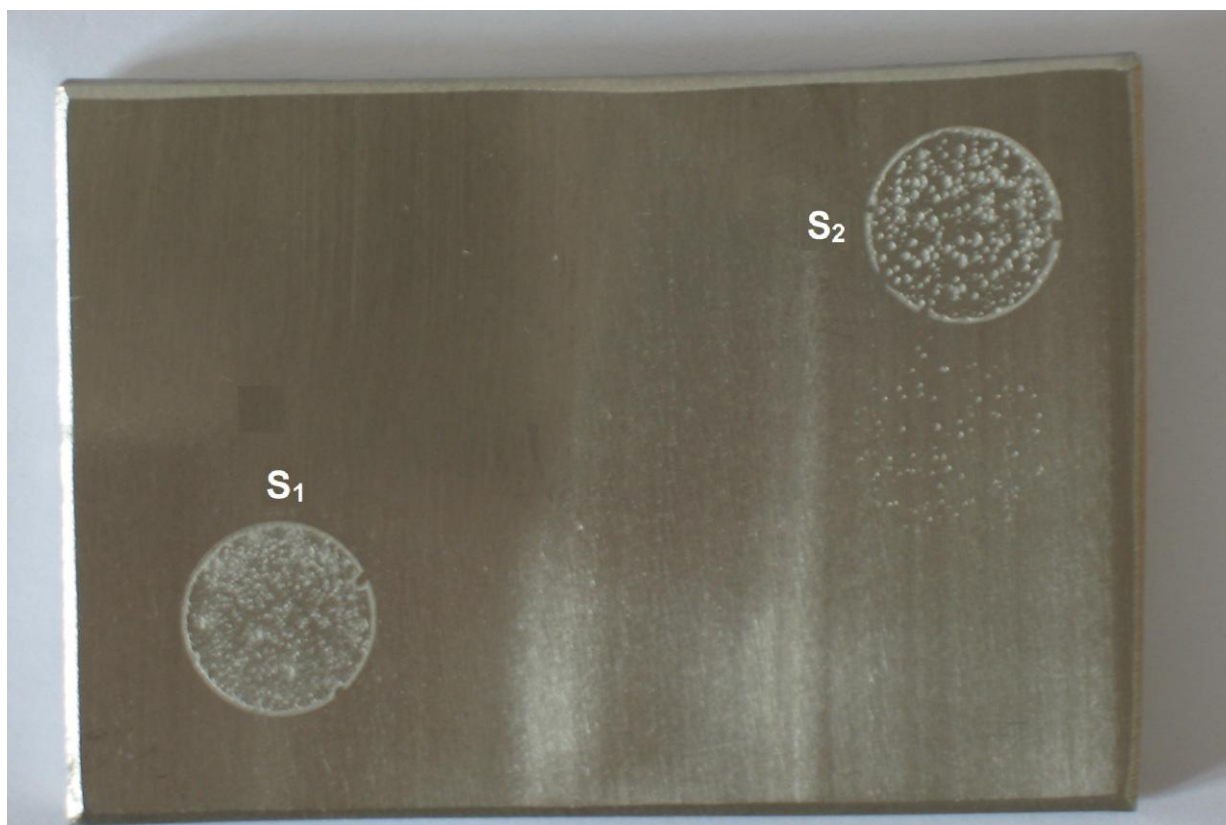

Figure 4. Clusters of corrosion micro-pits (confined within the working electrode: circular areas denoted as S_1 and S_2), induced upon anodic polarization experiments on the surface of welded-joint, 8 mm SS plate.

Furthermore, the corrosion performance of 316L SS weldments was monitored by the linear polarization method, where micro-polarizations were conducted at ± 15 mV around an open circuit/corrosion potential (ocp). The polarization resistance (R_p) parameter was calculated as the inverse of the slope of I (current) vs. E (potential) graph, based on the micro-polarization measurements (see Table 2 below). The relationship between corrosion current, I_{corr} and R_p parameters can be represented by the well-known Stern-Geary relationship (equation 6), which becomes simplified to $I_{corr} = 0.026\, R_p^{-1}$ when Tafel slopes (b_a and b_c) of 120 mV decade^{-1} are used.

$$(6) \qquad I_{corr} = \frac{b_a b_c}{2.303 R_p (b_a + b_c)}$$

Table 2. Calculated average values of resistance polarization (R_p) parameter for welded-joint 316L SS material.

pH	R_p (Ω cm^2)	
	Untreated sample	Passivated sample
2.0	2.1×10^5	4.7×10^5
6.5	6.8×10^5	3.4×10^6

Thus, the resistance polarization values of 2.1×10^5 and 6.8×10^5 Ω cm^2 (see Table 2) were recorded for the welded-joint 316L SS material in contact with 1.0 mol dm^{-3} NaCl, at pH 2.0 and 6.5, correspondingly (a relative increase of the R_p parameter by 3.2 times for pH 6.5 is observed). Again, the surface passivation treatment led to significant improvement of the corrosion performance, where the recorded R_ps for the passivated SS samples increased by *ca*. 2.2 and 5.0 times (in relation to the untreated specimens) for pH 2.0 and 6.5, respectively.

4. CONCLUSIONS

Extensive application of hypochlorite-based disinfecting reagent(s) to sanitize a 316L stainless steel-made dairy reactor contributed to the development of significant pitting, which was entirely confined to the welding zone of the reactor. As no evidence of pitting was found outside the welding area, it is strongly believed that the corrosion phenomenon is directly linked to improper employment of welding procedures (e.g. too rapid cooling, inefficient gas purge and/or poor post-welding cleaning). As a consequence, locally present surface defects, inclusions and other material inhomogeneities led to the formation of defected passive film over the welding zone of the SS material. This resulted in significant pitting corrosion, primarily initiated upon contact with a chloride (hypochlorite-derived upon *in-situ* ClO$^-$ disproportionation reaction at elevated temperatures) containing sanitizing solution. The above conclusion can be supported by the fact that significantly increased presence of δ-ferrite in the austenitic SS structure was observed for both heat-affected zone (about 8 %) and weld area (15 %), as compared to the virgin 316L stainless steel material. Here, significant content of δ-ferrite effected in greater susceptibility of the weld material to the pitting corrosion attack [10, 13].

Finally, a substantial improvement of the corrosion performance of 316L SS welded-joint material could be achieved through locally applied surface passivation treatment. The above resulted in a considerable strengthening of the surface passive film, thus providing enhanced protection against general and pitting corrosion, being especially evident at pH approaching neutral value.

References

1. M.G. Fontana, *Corrosion Engineering*, 3rd ed., McGraw-Hill, New York, 1987, Chapter 3, 63.
2. H.H. Uhlig, R.W. Revie, *Corrosion and Corrosion Control: An Introduction to Corrosion Science and Engineering*, 3rd ed., John Wiley & Sons, New York, 1985, Chapter 5, 74 and Chapter 18, 313.

3. P.R. Roberge, *Handbook of Corrosion Engineering*, McGraw-Hill, New York, 2000, Chapter 8, 733.
4. L. Odegard, *Welding in the World*, 36, (1995), 153.
5. *Corrosion of Weldments. Basic Understanding of Weld Corrosion*, ASM International, Materials Park, 2006, Chapter 1, 1, http://www.asminternational.org.
6. *Diversey – MSDS link*, http://www.johnsondiversey.com/Cultures/en-GB/Corporate+Information/MSDS.
7. A.B. Djordjevic, B.Z. Nikolic, I.V. Kadija, A.R. Despic, M.M. Jaksic, *Electrochim. Acta*, 18(7), (1973), 465.
8. S.B. Jonnalagadda, S. Nadupalli, *Talanta*, 64, (2004), 18.
9. A.V.C. Sobral, W. Ristow Jr., D.S. Azambuja, I. Costa, C.V. Franco, *Corros. Sci.*, 43, (2001), 1019.
10. C. Garcia, F. Martin, P. de Tiedra, Y. Blanco, M. Lopez, *Corros. Sci.*, 50, (2008), 1184.
11. T.Yamamoto, K. Fushimi, M. Seo, S. Tsuri, T. Adachi, H. Habazaki, *Corros. Sci.*, 51, (2009), 1545.
12. A.Rauf, W.F. Bogaerts, *Corros. Sci.*, 52, (2010), 2773.
13. E.M. Zahrani, A. Saatchi, A. Alfantazi, *Eng. Fail. Anal.*, 17, (2010), 810.